WATER RESOURCES RESEARCH, VOL. 25, NO. 10, PAGES 2149–2158, OCTOBER 1989

One-Dimensional Steady State Infiltration in Heterogeneous Soils

T.-C. JIM YEH

Department of Hydrology and Water Resources, University of Arizona, Tucson

The effects of heterogeneity on one-dimensional, steady state infiltration are studied using numerical simulations where the soil hydrologic properties are assumed to be spatial stochastic processes. Analytical solutions to one-dimensional, steady state infiltration in heterogeneous soils are developed and applied to the stochastic random fields. The effects of spatial variability of parameters of an exponential unsaturated hydraulic conductivity model on the soil-water pressure profiles are examined. The amount of variation in pressure heads is found to vary with infiltration rates and mean pressure heads, while the cross-correlation between parameters is shown to have important influences on the value of the head variance. An inverse procedure is developed to determine the effective hydraulic conductivity parameters. The effective parameter is found to vary with mean pressures. Effective hydraulic conductivities and pressure head variances estimated from the numerical simulations were compared with those obtained from a spectral method by Yeh et al. (1985a, b, c). A unit mean gradient approach was used to estimate the effective unsaturated hydraulic conductivity, and the result shows that this approach is adequate for heterogeneous soils.

INTRODUCTION

The spatial variability of soil hydrologic parameters has been recognized for years. *Nielsen et al.* [1973] and *Stockton and Warrick* [1971] showed that there is a large variation in hydraulic conductivity, moisture content, and other hydrologic property values in the field. Moreover, recent field studies of the spatial variability of soil properties by *Sisson and Wierenga* [1981], *Vieira et al.* [1981], *Russo and Bresler* [1980], *Byers and Stephens* [1983], *Yeh et al.* [1986*b*], and *Greenholtz et al.* [1988] demonstrated that spatial variations are not entirely random but are spatially correlated. The effects of spatial variability on flow and transport in unsaturated zones have recently been explored by many theoretical works [e.g., *Warrick et al.*, 1977; *Jury*, 1982; *Dagan and Bresler*, 1980; *Andersen and Shapiro*, 1983]. Studies by *Yeh et al.* [1985*a*, *b*, *c*] used the two-parameter exponential conductivity function introduced by *Gardner* [1958] to investigate the spatial variability of unsaturated flow. They treated the spatially varying hydraulic properties of unsaturated media as stochastic processes and used a spectral technique to derive the variance of soil-water pressure head and the effective hydraulic conductivity of stochastic random media under steady state infiltration conditions. The result of their studies showed that the head variance was mean-dependent and increased with mean soil-water pressure head (i.e., the drier the soil, the larger the head variance). The effective hydraulic conductivity was shown to be a second-rank tensor and anisotropic. The anisotropy is, however, moisture-dependent (i.e., the ratio of the horizontal to the vertical hydraulic conductivity depends on the soil water saturation). Such a moisture-dependent anisotropy is different from classic infiltration theories which generally assume the soil to be either isotropic or anisotropic with a constant ratio. They also emphasized the importance of the spatial variability of the "pore size distribution parameter" of the exponential model in the analysis of unsaturated flow in heterogeneous soils. *Mantoglou and Gelhar* [1987*a*, *b*, *c*] analyzed unsteady unsaturated flow in heterogeneous porous media. The results of their studies indicated that moisture-dependent anisotropy shows significant hysteresis, depending on the mean flow conditions (wetting or drying). Furthermore, both *Yeh et al.* [1985*a*, *b*, *c*] and *Mantoglou and Gelhar* [1987*a*, *b*, *c*] concluded that the moisture-dependent anisotropy due to heterogeneities can cause significant lateral migration of water and pollutants in heterogenous unsaturated zones.

Field soil-water pressure data collected by *Yeh et al.* [1986*b*] and *Greenholtz et al.* [1988] support the mean-dependent head variance concept. Additionally, results of laboratory experiments [Mathieu and Yeh, 1988; *Stephens and Heermann*, 1988] and field observations [*Crosby et al.*, 1968, 1971*a*, *b*; *Murphy et al.*, 1988] indicated large lateral migrations of pollutants and moisture in heterogeneous unsaturated soils.

Although these laboratory and field results support the moisture-dependent head variance and anisotropy concepts, a quantitative verification of these concepts is needed. The analyses by *Yeh et al.* [1985*a*, *b*, *c*] and *Mantoglou and Gelhar* [1987*a*, *b*, *c*] are approximations which used the assumption that perturbations in flow equations for heterogeneous media were small so that mathematics in the analysis could be simplified. The small perturbation assumption has been shown to be robust in saturated media [*Gutjahr*, 1984; *Ababou et al.*, 1988]. This assumption in unsaturated media is, however, subject to debate because the perturbation grows with the mean. For instance, the head variance increases as the soil becomes dry. Therefore it is necessary to assess the validity of the results derived from the perturbation analysis. Observations from many carefully designed field experiments are most appropriate, but these field experiments are generally rare. Numerical experiments are a possible alternative.

Ababou et al. [1988] conducted numerical simulations of three-dimensional steady state infiltration in media of random unsaturated hydraulic conductivity fields. They concluded that simulated head variance and effective conductivity compared well with the steady state spectral solution obtained by *Mantoglou and Gelhar* [1987*b*]. However, since a large number of nodes (300,000 nodes) were used in the simulation, their analysis was restricted to cases with a

Paper number 89WR01104.
0043-1397/89/89WR-01104$05.00

single realization of random unsaturated hydraulic conductivity fields with a specific infiltration rate. Monte Carlo simulations of two-dimensional, steady state unsaturated flow through autocorrelated random fields were conducted by *Hopmans et al.* [1988]. Only thin unsaturated zones (0.6–1.0 m) above the water table were considered; the simulation results may thus be influenced by the capillary fringe. Strictly speaking, their results cannot be compared with those by spectral methods which assume unit gradient situations. However, the results of their simulations support the general conclusions by *Yeh et al.* [1985*a*].

The purposes of this paper are to study the effects of heterogeneities on pressure profiles resulting from one-dimensional, steady state infiltration, to analyze the effective unsaturated hydraulic conductivity in heterogeneous soils, and to compare the head variance and the effective hydraulic conductivity estimated from the simulations to stochastic results developed by *Yeh et al.* [1985*a*, *b*, *c*]. Because of difficulties in solving two- and three-dimensional unsaturated flow equations, this study is limited to one-dimensional, steady state infiltration. Although one-dimensional, steady state infiltration may not closely represent field situations, it is, however, the first step to quantitatively test those stochastic results.

METHODS

Hydraulic Conductivity

Knowledge of the hydraulic conductivity and soil-water pressure head relationship of a porous medium is required to study unsaturated flow in the medium. In this study an exponential model [*Gardner*, 1958] was used for this relationship, that is,

$$K(\psi) = K_s \exp(\alpha\psi) \tag{1}$$

where $K(\psi)$ is the hydraulic conductivity, a function of the soil-water pressure head ψ (negative), and hysteresis is ignored. K_s is the hydraulic conductivity of the medium at $\psi = 0$, and α is the pore size distribution parameter which characterizes the rate of reduction in hydraulic conductivity as ψ becomes more negative.

For mathematical convenience, a log transform of (1) gives

$$\ln K(\psi) = \ln K_s + \alpha\psi \tag{2}$$

Equation (2) defines a linear relationship between ln K and α in which α is the slope and ln K_s is the intercept at $\psi = 0$. Since the assumed exponential model may or may not apply to a given soil type for the full range of soil-water pressure, the K_s value may or may not represent the saturated hydraulic conductivity of the medium. The appropriate definition of the parameters for a given soil may depend upon the range of the hydraulic conductivity pressure head data to which the model, (2), is applied. Generally, large values of K_s and α correspond to coarse materials such as sand and gravel, and small values represent fine-textured materials. Thus characterizing the hydraulic conductivity behavior of a porous medium under any soil-water pressure requires the knowledge of the values of these two parameters.

Generation of Random ln K_s and α Fields

Because of the heterogeneous nature of soil formations and the lack of complete knowledge of the spatial distribution of hydrologic properties of soil formations, it is appropriate to represent the parameters ln K_s and α as stochastic processes in space. Many field data [*Greenholtz et al.*, 1988; *Bakr*, 1976; *Russo and Bresler*, 1980, *Byers and Stephens*, 1983] showed that these parameters are not entirely random but spatially correlated. Therefore statistical properties such as joint probability distributions, means, variances, and correlation functions of the two parameters are required to characterize their spatial variability. This statistical information, however, does not specify any single spatial arrangement of these two parameter values. That is, for a given set of the statistical information there are many possible realizations of spatial arrangement of the ln K_s and α values. Therefore in order to produce a specific spatial arrangement of the soil hydrologic parameter values for the given statistics a one-dimensional random field generator was employed in this study.

The random field generator used here, capable of generating random fields with any given covariance function, is based on an algorithm formulated by *Albano* [1981]. This algorithm uses the spectral representation theorem [*Lumley and Panofsky*, 1964] which states that if $Y(x)$ is a second-order stationary stochastic process with zero mean and covariance $C(s)$, then there exists a unique complex stochastic process $dZ(\omega)$, such that

$$Y(x) = \int_{-\infty}^{\infty} \exp(i\omega x)\, dZ(\omega) \tag{3}$$

where $i = \sqrt{-1}$, and ω is the wave number. In addition, there exists a unique distribution function F such that

$$C(s) = \int_{-\infty}^{\infty} \exp(i\omega s)\, dF(\omega) \tag{4}$$

$$E[dZ(\omega_1)\, dZ^*(\omega_2)] = dF(\omega) \qquad \omega_1 = \omega_2$$

$$E[dZ(\omega_1)\, dZ^*(\omega_2)] = 0 \qquad \omega_1 \neq \omega_2$$

where $dZ^*(\omega)$ is the complex conjugate of dZ.

To use this theorem to generate a real-valued stochastic process, $Y(x)$, requires the knowledge of the covariance function $C(s)$ of the process. In this analysis, an exponential covariance function, $C(s) = \sigma^2 \exp(-|s|/l)$, was used, where σ^2 is the variance, s is the separation distance, and l is the integral scale. The spectral density corresponding to this function, which is the Fourier transform of the covariance, is

$$dF(\omega) = \frac{l}{\pi(1 + l^2\omega^2)} \tag{5}$$

and the spectral distribution function

$$F(\omega) = \frac{1}{\pi}(\tan^{-1} l\omega) + \frac{1}{2} \tag{6}$$

To generate the dZ, two independent, uniform, mean 0, variance 0.5, univariate random variables U and V are generated to represent the real part and imaginary part of the complex dZ process, respectively. This value is then multiplied by $(dF(\omega))^{1/2}$. The entire process is repeated for all ω, yielding a complex random vector dZ which satisfies both (3) and (4). The Fourier transform of the dZ process then produces the $Y(x)$ random field possessing the specified covariance function. The Fourier transform was carried out

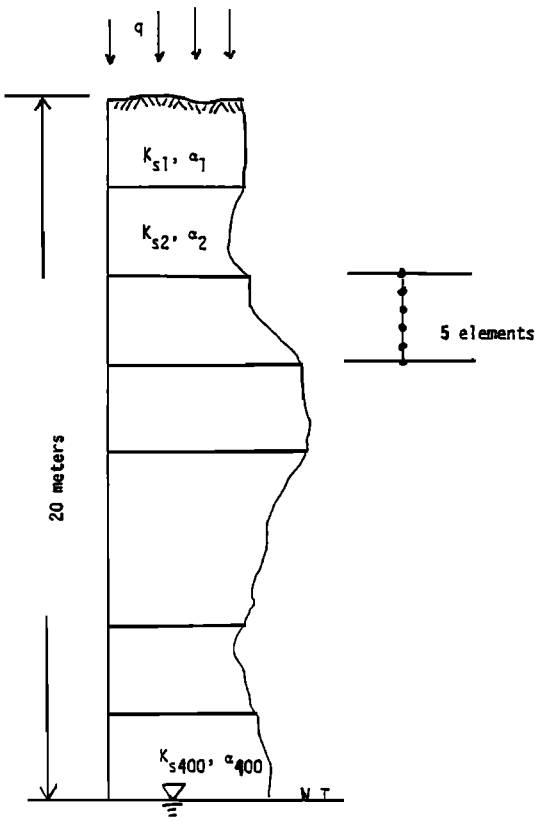

Fig. 1. The hypothetical soil profile and boundary conditions examined in this study.

by the fast Fourier transform algorithm in the work by *Press et al.* [1986].

The physical situation examined in this study was steady state infiltration into a 20-m-thick unsaturated soil formation. The formation consisted of 400 layers. Each layer was assigned a pair of ln K_s and α values and was discretized into five homogeneous soil blocks. The flow regime was assumed to be one-dimensional. The upper boundary was set to be a prescribed flux boundary condition, and the lower boundary was a stationary water table (Figure 1).

The parameters ln K_s and α were assumed to be second-order stationary stochastic processes with means F and A and perturbations f and a, respectively. Both ln K_s and α processes were synthesized using the procedure discussed above. Since two random processes were considered, the relationship between these two random processes must be specified. However, field data pertaining to the relationship between the two parameters are rare. In this study, two extreme cases were analyzed: case I, where ln K_s and α are perfectly correlated random fields, and case II, where ln K_s and α are treated as uncorrelated processes. In both cases the autocorrelation functions of the ln K_s and α processes were assumed to be exponential functions with identical integral scales.

A rigorous test of the stochastic results by *Yeh et al.* [1985*a*, *b*, *c*] requires conducting a Monte Carlo simulation which involves generating many realizations of random ln K_s and α fields. To avoid such a computation intensive and therefore time-consuming task, the ergodicity assumption was used. That is, the probability distribution of a single spatial realization can be viewed as that of the ensemble. The 400 pairs of ln K_s and α parameters (one value of ln K_s and α for each layer) were considered a large enough sample size for the ergodicity theorem to apply. Since data collected in a field represent a single realization of a stochastic process, the analysis based on a single realization of ln K_s and α processes in this study thus, in a sense, serves the purpose of testing the applicability of the stochastic results to field situations.

Analytical Solution

To determine the pressure head distribution in the generated random fields, an analytical solution was developed. For one-dimensional, steady state, vertical infiltration in a unsaturated homogeneous soil the specific discharge is given by

$$q = -K(\psi)\left[\frac{d\psi}{dz} + 1\right] \tag{7}$$

where a negative q represents infiltration. If the hydraulic conductivity and pressure head relationship is assumed to be described by (1), by integrating (7) [*Bear*, 1972] the soil-water pressure head becomes

$$\psi = \frac{1}{\alpha} \ln \left\{ \exp\left[-\alpha(z - \psi_0)\right] + \frac{q}{K_s} \exp\left(-\alpha z\right) - \frac{q}{K_s} \right\} \tag{8}$$

where z is the elevation, ψ_0 is the prescribed head at $z = 0$, and q is the flux at the land surface. Equation (8) is valid only if

$$0 < \left\{ \exp\left[-\alpha(z - \psi_0)\right] + \frac{q}{K_s} \exp\left(-\alpha z\right) - \frac{q}{K_s} \right\} \leq 1 \tag{9}$$

in other words, $\psi \leq 0$.

For layered soils, (8) can be applied to the lowest layer first to obtain the pressure head at the interface between this layer and the overlying layer. Since flow is steady, continuity requires that the pressure head in the lower layer equals that in the upper layer at the interface. The pressure head distribution in the overlying layer can thus be evaluated by using (8) and the pressure head at the interface as the prescribed head ψ_0 at the lower boundary of the overlying layer. Therefore using this procedure recursively, one can easily obtain the pressure profile distribution in a formation containing any number of layers.

Inverse Procedure

The effective hydraulic conductivity of the synthesized heterogeneous soil formation was derived by conceptualizing the soil formation as an equivalent homogenous medium. Under the same boundary conditions the equivalent homogeneous medium will discharge the same amount of flux as the heterogeneous one. It follows then that the K-ψ relationship of this equivalent homogeneous medium is the effective K-ψ relationship of the heterogeneous medium. For simplicity, this effective hydraulic conductivity and pressure relationship is assumed to be exponential, as in equation (1). Thus the effective parameters for characterizing the medium are $\hat{K}_s$ and $\hat{\alpha}$, where the circumflex denotes an effective parameter. If these two parameter values are known, (8)

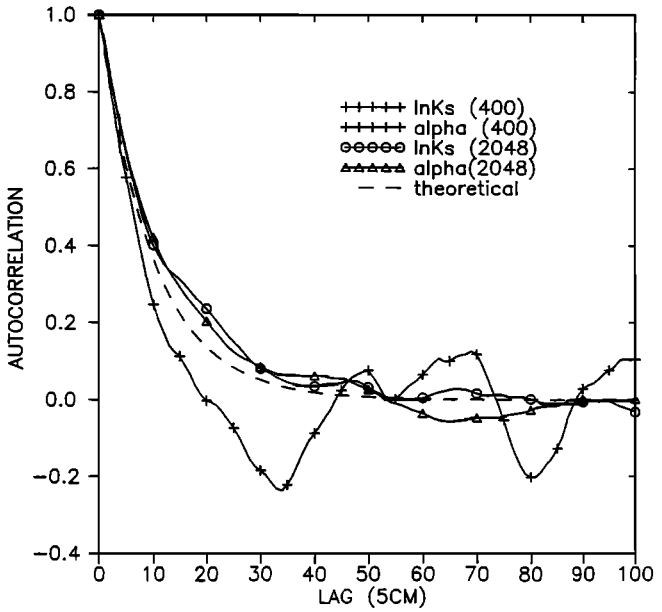

Fig. 2. Autocorrelation functions of ln K_s and α processes, estimated from 400 and 2048 generated values.

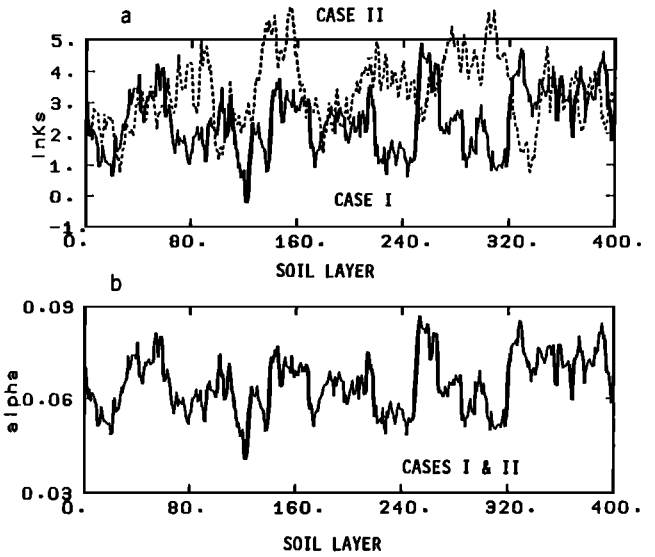

Fig. 3. (*a*) Spatial distributions of the ln K_s and (*b*) α values in cases I and II.

describes the pressure head distribution in the equivalent homogenous medium. Further, if the infiltration rate is specified, substitution of the effective parameters in (8) will produce the mean pressure head distribution in the heterogeneous soil such that

$$\sum_{i=1}^{n} (H_i - \psi_i)^2 = \text{minimum} \qquad (10)$$

where H_i is the pressure head value at ith depth calculated by (8) with the effective parameters, ψ_i is the pressure head in the heterogeneous soil at ith depth, and n is the total number of depths. Inasmuch as the effective parameters $\hat{K}_s$ and $\hat{\alpha}$ are unknown, (8) was regressed against ψ values with the aid of the Levenberg-Marquardt method [*Press et al.*, 1986] to reach the condition (10). The parameter values providing the best fit were considered as the effective parameter values.

Results

For case I (ln K_s and α are perfectly correlated) the mean and the variance of ln K_s were specified to be 3.0 and 1.2, respectively, while the mean and the variance of α were 0.07 cm^{-1} and 0.0001 cm^{-2}, respectively. These values correspond to silty clay loam [*Yeh et al.*, 1985*c*]. An exponential covariance function with an integral scale of 50 cm (10 layers) was assumed. Since ln K_s and α are assumed to be perfectly correlated, the same seed was used. Two thousand forty-eight pairs of ln K_s and α values were generated by the spectral method discussed previously. The sample mean and variance of the ln K_s process from the generated data were 2.91 and 1.31, respectively. The sample mean of the α process was 0.069 cm^{-1}, and the variance was 0.00011 cm^{-2}. The estimated autocorrelation functions for ln K_s and α processes are shown in Figure 2. However, only the first 400 pairs of ln K_s and α values were assigned to the 400 layers of the soil formation. Figures 3*a* and 3*b* show the spatial distribution of ln K_s and α values along the vertical. The correlation between ln K_s and α processes was checked graphically by plotting ln K_s versus α. A perfect linear relationship between these processes with a slope of −109 cm was found, indicating a perfect correlation between the two process. The estimated autocorrelation functions from the 400 data values are also shown in Figure 2.

For case II where ln K_s and α are uncorrelated, 2048 ln K_s values were regenerated with the same mean and variance as in case I but with a seed value different from that in case I. The same covariance function as in case I was used. The estimated mean and variance of the ln K_s process were 2.97 and 1.36, respectively. For the α random field the same realization generated in case I was used. The estimated autocorrelation function for the new ln K_s process is identical to that of case I. Again, the first 400 pairs of ln K_s and α values were assigned to the layers of the soil formation (Figures 3*a* and 3*b*). The independence of ln K_s and α was checked by plotting ln K_s versus α values. No noticeable relationship between ln K_s and α was found, indicating independence of ln K_s from α.

Since the analytical solution (8) is valid for unsaturated situations only, it was then applied to the synthesized heterogeneous soil to obtain soil-water pressure head profiles under six different infiltration rates (i.e., q = −1.0, −0.1, −0.006, −0.002, −0.0005, and −0.0001 cm/d). These infiltration rates were used to ensure unsaturated conditions along the entire profiles. These calculated pressure head profiles for both cases are illustrated in Figures 4 and 5 as a function of depth.

Analysis of Results and Discussions

Pressure Head Variance

Figure 4 shows the simulated pressure head distribution with depth in case I (ln K_s and α perfectly correlated). Pressure head values fluctuated significantly with depth. To objectively determine the mean pressure head profile at each

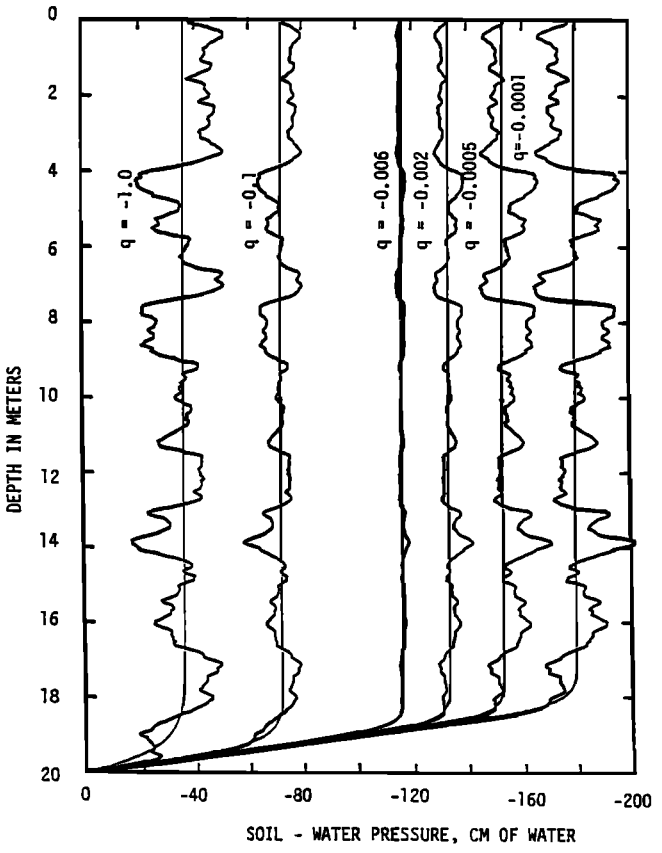

Fig. 4. Simulated soil-water pressure head distributions for perfectly correlated ln K_s and α (case I) under six infiltration rates.

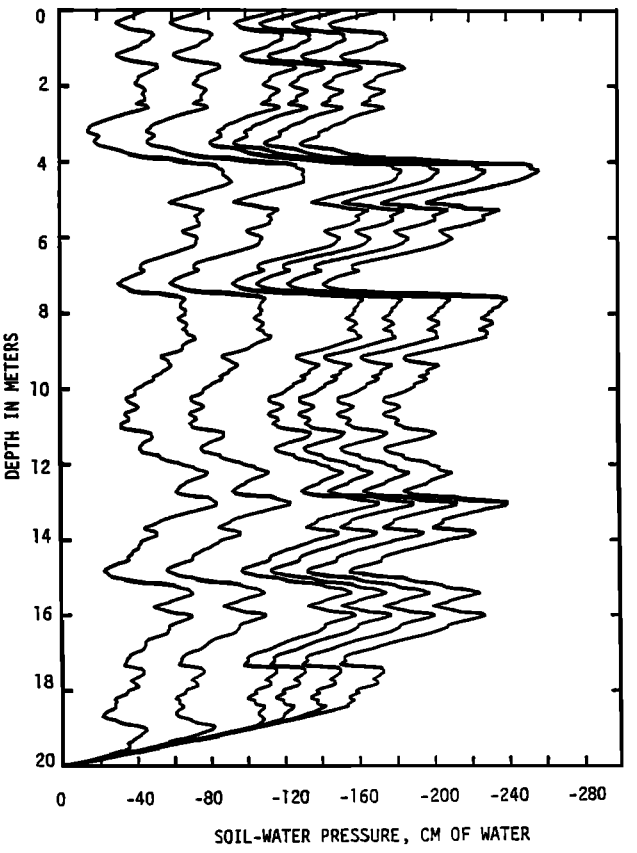

Fig. 5. Simulated soil-water pressure head distributions for uncorrelated ln K_s and α (case II) under six infiltration rates.

infiltration rate the inverse procedure was employed. The solid smooth curves in Figure 4 are the resultant mean pressure head profiles under different infiltration rates. These smooth mean pressure head profiles show that for a large portion of the soil formation, mean pressure head values reach a unit gradient situation. It is seen that the variability of head values as shown in the figure tends to decrease as the infiltration rate decreases. A nearly uniform head distribution was obtained as the infiltration rate approached 0.006 cm/d. However, the pressure head variation increased again after the infiltration rate became less than 0.006 cm/d. Figure 4 also shows that the wet regions at large infiltration rates became dry regions after the infiltration rate decreased from 0.006 cm/d and vice versa. The profiles appear to be symmetrical about the profile, resulting from a infiltration rate of 0.006 cm/d (a mirror image effect).

The pressure head profiles for six different infiltration rates in case II, where ln K_s and α are uncorrelated, are illustrated in Figure 5. The profiles are significantly different from those in case I. The variation in pressure head values grew as the infiltration rate decreased.

Note that variability in head is minimal near the water table in both cases. This can be attributed to the capillary fringe effect. It is also found that the pressure head in both cases tends to be normally distributed.

Before explaining the results of the pressure head profiles in cases I and II, it is necessary to examine the physical situation that cases I and II represent. Figure 6*a* illustrates the ln K and ψ relationships for the case where ln K_s and α are correlated. Because of the perfect correlation between ln K_s and α processes (i.e., soil with a large value of ln K_s has a large value of α or slope of the ln K-ψ relationship and vice versa), all the ln K-ψ curves intersect at the soil-water pressure head equal to the constant of proportionality between ln K_s and α, which is about -109 cm. This constant represents the ratio of the standard deviation of ln K_s to that of α. On the other hand, the ln K-ψ relationships for the uncorrelated case do not exhibit this unique property (Figure 6*b*), since all the ln K-ψ curves tend to diverge as ψ becomes more negative.

By examining Figures 6*a* and 6*b*, one should be able to explain the differences between the results of case I and case II. In case I, at the infiltration rate of 1.0 cm/d, the mean pressure head was about -35 cm at the portion of the soil formation where unit mean gradient existed. Since the mean profile approached a constant value, the infiltration rate was equal to the hydraulic conductivity at that mean pressure head value. If one draws a line parallel to the pressure head axis in Figure 6*a* at $K = 1$ cm/d, this line will intersect with all the ln K-ψ curves. If one assumes that a unit gradient condition exists over the large portion of each layer, the length of the line segment A-B bounded by two outermost ln K-ψ curves (one with the largest α value and the other the smallest) represents the variation in pressure head. It is evident from the figure that as the K values decrease, the length of the segment will decrease. The length of the segment approaches zero as K becomes close to 0.006 cm/d because all the ln K-ψ curves cross at that infiltration rate or a mean pressure value of -109 cm. As a result, the variation in ψ becomes minimal. Once the infiltration rate drops

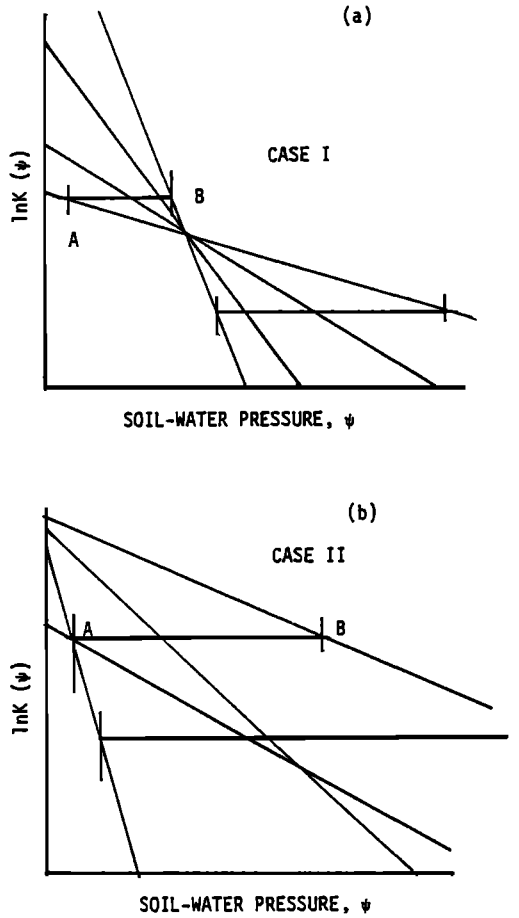

Fig. 6. A schematic illustration of ln K-ψ relationships in (*a*) case I and (*b*) case II.

beyond this rate, the length of the segment or the variability in ψ begins to grow again.

The symmetrical nature of the profiles is also related to the perfect correlation between ln K_s and α. At pressures less than -109 cm, as shown in Figure 6*a*, the layers with smaller α values (fine-textured materials) are more conductive than those with large α values. Therefore in order to maintain the same flux to satisfy the steady state condition the pressure values in fine-textured materials have to be much greater than those of coarse-textured materials. This explains the mirror image effect of pressure head profiles in case I under six different infiltration rates.

On the other hand, the length of the segment A-B in Figure 6*b* grows as the infiltrate rate or ln K value decreases. This is due to the fact that the ln K-ψ curves in this case tend to diverge as the pressure head becomes more negative. The increasing variability in pressure head in case II as infiltration rate decreases may thus become clear.

The pressure head profiles in cases I and II, calculated by the analytical solution, are exact. They provide a means to quantitatively test the stochastic result by *Yeh et al.* [1985*b*]. The comparison was carried out by using equations (5.2.14) and (5.2.19) in the work by *Yeh* [1983]. That is, for the case where ln K_s and α are perfectly correlated, the head variance is given as

$$\sigma_\psi^2 = \frac{\sigma_f^2 l^2 (1 + H\xi)^2}{Al((1 + Al))} \tag{11}$$

For uncorrelated ln K_s and α, the head variance is

$$\sigma_\psi^2 = \frac{(\sigma_f^2 + \sigma_\alpha^2 H^2) l^2}{Al((1 + Al))} \tag{12}$$

where H is the mean soil-water pressure head (negative), and l is the integral scale of the ln K_s and α parameters. The constant of proportionality between α and ln K_s is ξ while σ_f^2 and σ_α^2 are the variance of ln K_s and α, respectively. The "A" denotes the mean of α. Note that (11) and (12) were derived with the assumption that the mean hydraulic gradient equals to unity.

To calculate the head variance using (11) and (12), the values of the means and variances of the ln K_s and α processes estimated from the 400 and the 2048 generated values were used. For the 400 ln K_s and α values, the estimated F (the mean of ln K_s) and σ_f^2 are 2.406 and 0.965, and 3.314 and 1.184 for case I and case II, respectively. The estimated A and σ_α^2 for both cases are 0.0646 cm^{-1} and 0.00008 cm^{-2}. These statistical parameters for the 2048 ln K_s and α values were reported earlier. Since (11) and (12) are limited to unit gradient situations, the mean head values in (11) are those at the portion of the simulated profiles where unit mean gradient exists. The mean head values in both cases were taken to be the arithmetic mean of the head values at sections of the soil profile where the mean gradient was visually considered as unity, excluding those head values near the water table. These mean head values agreed with those obtained by the inverse procedure. The remaining parameters to be determined are the integral scales l of the ln K_s and α parameters. The integral scales of both parameters were assumed to be the same, and they were estimated from their sample autocorrelation functions as the separation distance at which the autocorrelation value drops to e^{-1} level. Although autocorrelation function calculated from 400 generated values oscillated significantly, a relatively smooth autocorrelation function was obtained from all of the 2048 values (Figure 2). The integral scale estimated from 400 data points and 2048 data points, was 42 and 60 cm, respectively. These values are comparable with the integral scale, 50 cm, specified in the random field generation. Using the means, variances, and integral scales estimated from both the 400 and the 2048 ln K_s and α data, head variances at the six mean head values corresponding to the six infiltration rates were calculated using (11) for case I and (12) for case II. As shown in Figure 7, the head variances calculated by using (11) and (12) agreed with those obtained from the simulation. Overall, head variances determined using means, variances, and integral scales estimated from the 2048 series tend to match the simulated results better.

Effective Hydraulic Conductivity

The effective hydraulic conductivity in case I was first estimated by using the inverse procedure, with the assumption that the exponential hydraulic conductivity model (1) is valid for the effective hydraulic conductivity of the equivalent homogeneous porous medium. The inverse procedure then determined the effective $\hat{K}$ and $\hat{\alpha}$ values. These values are listed in Table 1 along with the six infiltration rates.

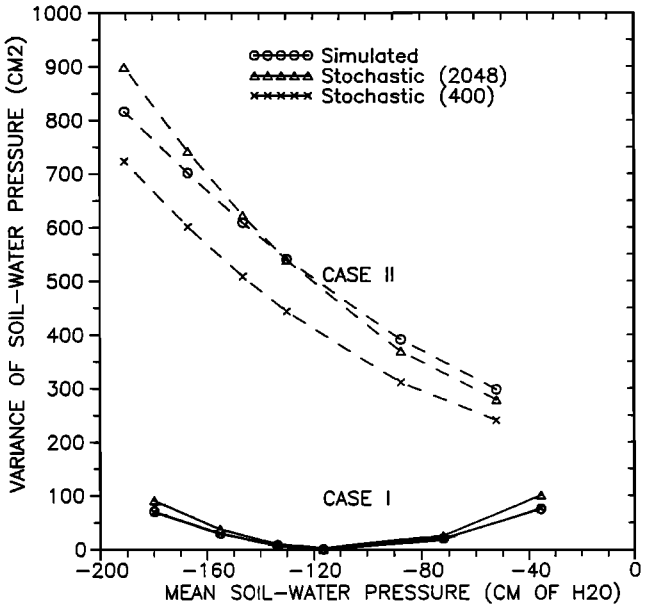

Fig. 7. Comparison of head variances simulated and those by *Yeh et al.* [1985*a*, *b*, *c*], with parameter values estimated from 400 and 2048 series for both case I and case II (dashed curve).

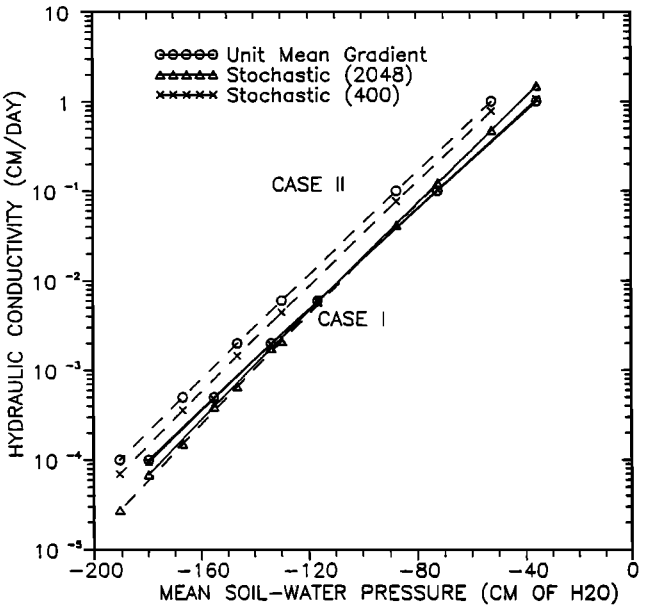

Fig. 8. Comparison of effective hydraulic conductivities derived from the unit mean gradient approach and those by the stochastic formula with parameter values estimated from 400 and 2048 series for case I and case II (dashed curve).

Values of these effective parameters tend to vary with infiltration rates without any noticeable pattern. Furthermore, the estimated $\hat{K}_s$ values are much smaller than the K_s values generated. This result can be attributed to the tradeoff between the effective $\hat{K}_s$ and $\hat{\alpha}$ values in the inverse process. Apparently, there is no unique combination of $\hat{K}_s$ and $\hat{\alpha}$ for the effective hydraulic conductivity.

An alternative of the inverse procedure for determining the effective ln K-ψ relationship is a unit mean gradient approach. This approach can be applied here because the mean head profiles in the large part of the soil formation were close to the unit gradient condition (Figures 4 and 5). Under the unit gradient assumption the hydraulic conductivity equals the infiltration rate at the corresponding mean pressure head. These pairs of hydraulic conductivity and mean pressure head values thus define the effective ln K-ψ relationships for both cases, and they are plotted in Figure 8. The effective hydraulic conductivity and pressure head relationships of both cases behave as an exponential function as the mean pressure head changes. For case I the estimated effective α and ln K_s are 0.063 cm^{-1} and 2.27, respectively. The effective K_s value is less than the geometric mean of K_s, and the effective α value is in agreement with the arithmetic mean of the 400 α values. Mean head profiles produced by the six infiltration rates in case I were also calculated using the analytical solution (8) with the effective parameters. Figure 9 illustrates the comparison of these profiles with those obtained by the inverse procedure. Overall, the head profiles calculated with the effective parameters agree with those obtained by the inverse procedure.

TABLE 1. Effective Hydraulic Conductivity Parameters for Case I, Estimated by the Inverse Procedure

Infiltration Rate, cm/d	$\hat{K}_s$, cm/d	$\hat{\alpha}$, cm^{-1}
1.0	2.096	0.0206
0.1	1.639	0.0386
0.006	4.480	0.0568
0.002	2.404	0.0531
0.0005	2.217	0.0542
0.0001	0.518	0.0476

The effective ln K-ψ relationships derived by the unit mean gradient approach were also compared to the formula derived on the basis of the results from *Yeh* [1983] and [*Yeh et al.*, 1986*a*]. For case I, where ln K_s and α are perfectly correlated, the formula for the effective unsaturated hydraulic conductivity K_e (H) is

$$K_e(H) = \hat{K}_s \exp(\hat{\alpha} H) \tag{13}$$

where

$$\hat{K}_s = \exp\left[F - \frac{\sigma_f^2}{2(1 + Al)}\right] \tag{14}$$

representing the hydraulic conductivity of the medium at zero mean soil-water pressure head, $H = 0$, and

$$\hat{\alpha} = \left\{A - \frac{[\sigma_f^2(H^2\xi^2 + 2H\xi) + 2\sigma_\alpha^2(H\xi + 1)l/\xi]}{2(1 + Al)H}\right. \tag{15}$$

where $\xi^2 = \sigma_\alpha^2/\sigma_f^2$ and $H < 0$. Similarly, for case II where ln K_s and α are uncorrelated, the effective hydraulic conductivity can be expressed as (13) with $\hat{K}_s$ identical to (14), but with

$$\hat{\alpha} = A - \frac{\sigma_\alpha^2(2l + H)}{2(1 + Al)} \tag{16}$$

The parameter values used to evaluate the effective hydraulic conductivities for both cases (equations (13)–(16)) were the same as those in the head variance analysis. Figure 8 shows that the predicted effective hydraulic conductivity curves using (13)–(16) are in close agreement with those

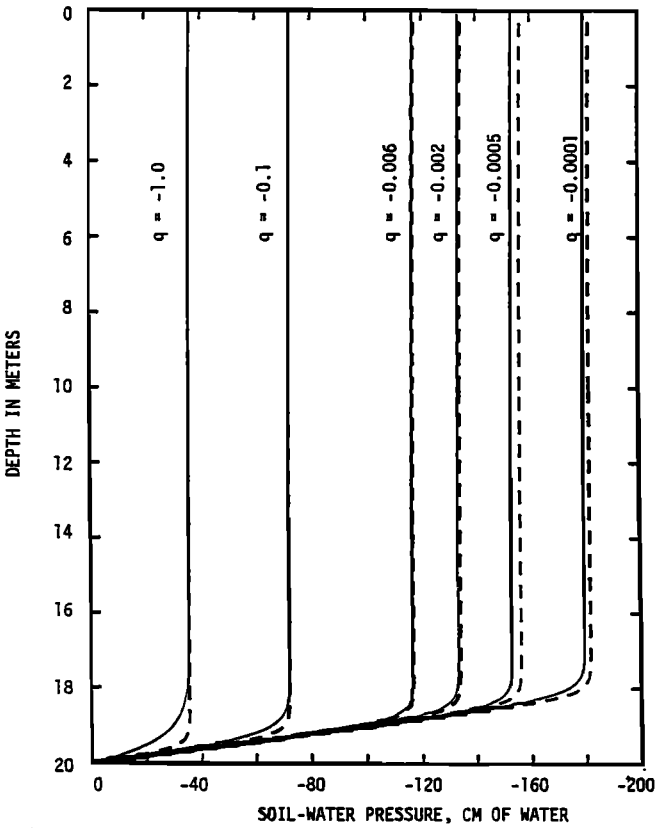

Fig. 9. Comparison of mean head profiles obtained by the inverse approach and those simulated with the effective hydraulic conductivity obtained by the unit mean gradient approach (dashed lines).

obtained from the unit mean gradient approach. For case II the effective hydraulic conductivity determined by the stochastic formula and the parameters estimated from the 2048 series, however, deviates substantially from that determined by the unit mean gradient approach. Interestingly, as shown previously, the parameter values estimated from the 2048 series gives a better result in terms of head variances. The discrepancy can be attributed to the fact that the head variances in case II are much greater than those in case I. The exponential generalization used in the spectral method [*Yeh et al.*, 1985*a*] to derive the effective hydraulic conductivity may fail at these large variances [*Poley*, 1988].

As mentioned earlier, the effective $\hat{K}_s$ and $\hat{\alpha}$ values estimated by the inverse procedure in case I at different infiltration rates tend to behave randomly. This indicates a compensation effect between the two parameters during the optimization process and no unique optimal values. However, according to the stochastic result (14), $\hat{K}_s$ values for both case I and case II can be expressed in terms of F, σ_f^2, A, and l. This implies that the $\hat{K}_s$ value depends on the properties of porous media only. Therefore it is reasonable to hold $\hat{K}_s$ constant while the inverse procedure is used to search for the effective parameter, $\hat{\alpha}$. On the basis of this assumption the $\hat{K}_s$ values were calculated using (14) and parameter values estimated from the 400 series as 9.73 and 23.41 cm/d for case I and case II, respectively. Since $\hat{K}_s$ is fixed, and $\hat{\alpha}$ is the only parameter to be searched, the trade-off between $\hat{K}_s$ and $\hat{\alpha}$ is thus eliminated. Table 2 tabulates the estimated $\hat{\alpha}$ values for the six infiltration rates

TABLE 2. Comparisons of the Effective Parameter $\hat{\alpha}$ Values Obtained by the Inverse Procedure and Stochastic Results

Infiltration Rate, cm/d	$\hat{\alpha}$ (Inverse), cm^{-1}	$\hat{\alpha}$ (Stochastic), cm^{-1}
	Case I	
1.0	0.06411	0.06447
0.1	0.06336	0.06344
0.006	0.06345	0.06340
0.002	0.06357	0.06348
0.0005	0.06375	0.06361
0.0001	0.06395	0.06379
	Case II	
1.0	0.06284	0.06424
0.1	0.06384	0.06463
0.006	0.06459	0.06509
0.002	0.06481	0.06527
0.0005	0.06506	0.06550
0.0001	0.06530	0.06576

in both case I and case II. These values were also compared to those obtained by using (15) and (16) (Figure 10). The stochastic results agree reasonably well with those obtained by the inverse procedure. Again, the discrepancy in case II is larger than in case I. This is again due to the larger head variance in case II than in case I. Errors due to extrapolating the hydraulic conductivity to large variances using the exponential approach in the spectral analysis thus become large.

It is also interesting to note that both (15) and (16), and the simulation results, indicate that the effective $\hat{\alpha}$ parameter value is not constant for a given heterogeneous porous medium but varies with mean pressure head. However, the dependence of $\hat{\alpha}$ on the mean pressure head does not seem to have significant effect on the overall effective hydraulic conductivity-pressure relationship, as shown in Figure 8.

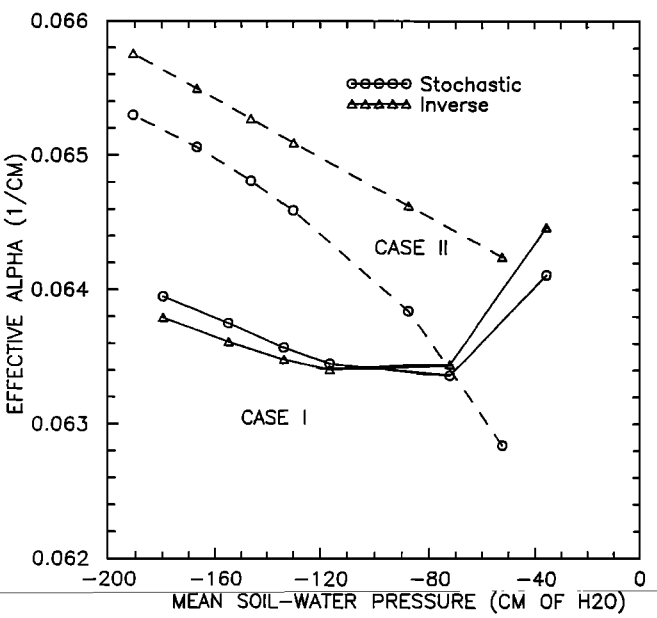

Fig. 10. Comparison of effective parameter $\hat{\alpha}$ derived from the inverse procedure and stochastic results, with the parameter values estimated from the 400 series for case I and case II (dashed curves).

CONCLUSIONS

In this study, pressure head profiles for one-dimensional steady state infiltration in unsaturated heterogeneous soils were calculated using analytical solutions. The analytical approach provides an easy way to demonstrate the effect of spatial variability in unsaturated hydraulic conductivity on unsaturated flow and to test the stochastic results developed by *Yeh et al.* [1985*a*, *b*, *c*]. Since the solution is exact, no iteration is required and no convergence problems exist, as in most numerical methods.

The results of the simulations illustrate the importance of considering the spatial variability of the ln K_s and α parameters in the analysis of unsaturated flow. The change in the variance of the pressure head with different infiltration rates seems to be largely related to the variance of the slope of K-ψ relationships or α parameters. In addition, the cross-correlation between ln K_s and α parameters can significantly affect the flow behaviors.

Effective unsaturated hydraulic conductivity of heterogeneous media with random K_s and α fields may not be represented by the exponential model. If the exponential model is used to describe the effective hydraulic conductivity and mean pressure head relationship, the effective $\hat{\alpha}$ parameter may vary with mean pressure head and variability of ln K_s and α at local scales.

The results of this study also indicate that the unit mean gradient approach is suitable for determining effective unsaturated hydraulic conductivities of heterogeneous porous media under steady state infiltration conditions. However, many soil-water pressure measurements are required in order to properly define the mean pressure.

The results of the study are in good agreement with the stochastic results obtained by *Yeh et al.* [1985*a*, *b*, *c*]. However, to fully test the robustness of their results may require a more rigorous analysis in which large values of the variances of ln K_s and α should be used, and many more realizations should be considered. Before a rigorous analysis is conducted, there is a need to quantify the range of the variability of the parameters (such as K_s and α) of unsaturated hydraulic conductivity models in various geologic environments. Finally, many carefully controlled field experiments will serve as the ultimate test of their hypotheses.

Acknowledgment. This research was supported by a grant from the National Science Foundation (CEE-8696060).

REFERENCES

Ababou, R., and L. W. Gelhar, Three-dimensional groundwater flow in random media, *M.I.T. Rep. 318*, 833 pp., Mass. Inst. of Technol., Cambridge, March 1988.

Albano, J. S., Simulation of stochastic processes, Masters thesis, Dep. of Math., N. M. Inst. of Min. and Technol., Socorro, July 1981.

Andersen, J., and A. M. Sharpiro, Stochastic analysis of one-dimensional steady state unsaturated flow: A comparison of Monte Carlo and perturbation methods, *Water Resour. Res.*, *19*(1), 121–133, 1983.

Bakr, A. A., Stochastic analysis of the effect of spatial variation in hydraulic conductivity on groundwater flow, Ph.D. dissertation, N.M. Inst. of Min. and Technol., Socorro, July 1976.

Bear, J., *Dynamics of Fluids in Porous Media*, 764 pp., Elsevier, New York, 1972.

Byers, E., and D. B. Stephens, Statistical and stochastic analysis of hydraulic conductivity and particle size in a fluvial sand, *Soil. Sci. Soc. Am. J.*, *47*, 1072–1080, 1983.

Crosby, J. W., D. J. Johnstone, C. H. Drake, and R. L. Fenston, Migration of pollutants in a glacial outwash environment, 1, *Water Resour. Res.*, *4*(5), 1095–1113, 1968.

Crosby, J. W., D. J. Johnstone, C. H. Drake, and R. L. Fenston, Migration of pollutants in a glacial outwash environment, 2, *Water Resour. Res.*, *7*(1), 204–208, 1971*a*.

Crosby, J. W., D. J. Johnstone, C. H. Drake, and R. L. Fenston, Migration of pollutants in a glacial outwash environment, 3, *Water Resour. Res.*, *7*(3), 713–720, 1971*b*.

Dagan, G., and E. Bresler, Solute dispersion in unsaturated heterogeneous soil at field scale: Theory, *Soil Sci. Soc. Am. J.*, *43*, 461–467, 1980.

Gardner, W. R., Some steady-state solutions of the unsaturated moisture flow equation with application to evaporation from a water table, *Soil Sci.*, *85*(4), 1958.

Greenholtz, D. E., T.-C. J. Yeh, M. S. B. Nash, and P. J. Wierenga, Geostatistical analysis of soil hydrologic properties in a field plot, *J. Contam. Hydrol.*, *3*(2–4), 227–250, 1988.

Gutjahr, A., Stochastic models of subsurface flow: Log linearized Gaussian models are "exact" for covariances, *Water Resour. Res.*, *20*(12), 1909–1912, 1984.

Hopmans, J. W., H. Schukking, and P. J. J. F. Torfs, Two-dimensional steady-state unsaturated water flow in heterogeneous soils with autocorrelated soil hydraulic properties, *Water Resour. Res.*, *24*(12), 2005–2017, 1988.

Lumley, J. L., and H. A. Panofsky, *The Structure of Atmospheric Turbulence*, 239 pp., John Wiley, New York, 1964.

Jury, W. A., Simulation of solute transport using a transfer function model, *Water Resour. Res.*, *18*(2), 363–368, 1982.

Mantoglou, A., and L. W. Gelhar, Stochastic modeling of large-scale transient unsaturated flow systems, *Water Resour. Res.*, *23*(1), 37–46, 1987*a*.

Mantoglou, A., and L. W. Gelhar, Capillary tension head variance, mean soil moisture content, and effective specific soil moisture capacity of transient unsaturated flow in stratified soils, *Water Resour. Res.*, *23*(1), 47–56, 1987*b*.

Mantoglou, A., and L. W. Gelhar, Effective hydraulic conductivities of transient unsaturated flow in stratified soils, *Water Resour. Res.*, *23*(1), 57–68, 1987*c*.

Mathieu, J. T., and T.-C. J. Yeh, Experimental investigation of seepage through heterogeneous media, *Tech. Rep. 88-010*, 71 pp., Dep. of Hydrol. and Water Resour., Univ. of Ariz., Tucson, October 1988.

Murphy, E. C., A. E. Kehew, G. H. Groenewold, and W. A. Beal, Leachate generated by an oil-and-gas brine pond site in North Dakota, *Ground Water*, *26*(1), 31–38, 1988.

Nielsen, D. R., J. W. Biggar, and K. T. Erh, Spatial variability of field measured soil-water properties, *Hilgardia*, *42*(7), 215–260, 1973.

Poley, A. D., Effective permeability and dispersion in locally heterogeneous aquifers, *Water Resour. Res.*, *24*(11), 1921–1926, 1988.

Press, W. H., B. P. Flannery, S. A. Teukilsky, and W. T. Vetterling, *Numerical Recipes, The Art of Scientific Computing*, 818 pp., Cambridge University Press, London, 1986.

Russo, D., and E. Bresler, Soil hydraulic properties as stochastic processes, 1, Analysis of field spatial variability, *Soil Sci. Soc. Am. J.*, *45*, 682–687, 1980.

Sisson, J. B., and P. J. Wierenga, Spatial variability of steady infiltration rates as a stochastic processes, *Soil Sci. Soc. Am. J.*, *45*, 699–704, 1981.

Stephens, D. B., and S. Heermann, Dependence of anisotropy on saturation in a stratified sand, *Water Resour. Res.*, *24*(5), 770–778, 1988.

Stockton, J. G., and A. W. Warrick, Spatial variability of unsaturated hydraulic conductivity, *Soil Sci. Soc. Am. J.*, *35*, 847–848, 1971.

Vieira, S. R., D. R. Nielsen, and J. W. Biggar, Spatial variability of field measured infiltration rates, *Soil Sci. Soc. Am. J.*, *45*, 1040–1048, 1981.

Warrick, A. W., G. J. Mullen, and D. R. Nielsen, Predictions of the soil water flux based upon field-measured soil-water properties, *Soil Sci. Soc. Am. J.*, *41*(1), 14–18, 1977.

Yeh, T.-C. J., Stochastic analysis of effects of spatial variability on

unsaturated flow, Ph.D. dissertation, 249 pp., N.M. Inst. of Min. and Technol., Socorro, 1983.
Yeh, T.-C. J., L. W. Gelhar, and A. L. Gutjahr, Stochastic analysis of unsaturated flow in heterogeneous soils, 1, Statistically isotropic media, *Water Resour. Res.*, *21*(4), 447–456, 1985a.
Yeh, T.-C. J., L. W. Gelhar, and A. L. Gutjahr, Stochastic analysis of unsaturated flow in heterogeneous soils, 2, Statistically anisotropic media with variable α, *Water Resour. Res.*, *21*(4), 457–464, 1985*b*.
Yeh, T.-C. J., L. W. Gelhar, and A. L. Gutjahr, Stochastic analysis of unsaturated flow in heterogeneous soils, 3, Observations and applications, *Water Resour. Res.*, *21*(4), 465–472, 1985*c*.
Yeh, T.-C. J., L. W. Gelhar, and A. L. Gutjahr, Correction to "Stochastic analysis of unsaturated flow in heterogeneous soils, 1 and 2," *Water Resour. Res.*, *25*(4), 843, 1986*a*.
Yeh, T.-C. J., L. W. Gelhar, and P. J. Wierenga, Observations of spatial variability so soil-water pressure in a field soil, *Soil Sci.*, *142*(1), 7–12, 1986*b*.

T.-C. J. Yeh, Department of Hydrology and Water Resources, University of Arizona, Tucson, AZ 85721.

(Received January 31, 1989;
revised May 22, 1989;
accepted May 26, 1989.)